Minireview

Solution NMR studies of the integral membrane proteins OmpX and OmpA from *Escherichia coli*

César Fernández*, Christian Hilty, Sophie Bonjour, Koba Adeishvili, Konstantin Pervushin[1], Kurt Wüthrich

Institut für Molekularbiologie und Biophysik, Eidgenössische Technische Hochschule Hönggerberg, CH-8093 Zürich, Switzerland

Received 11 July 2001; accepted 23 July 2001

First published online 6 August 2001

Edited by Andreas Engel and Giorgio Semenza

Abstract Membrane proteins are usually solubilized in polar solvents by incorporation into micelles. Even for small membrane proteins these mixed micelles have rather large molecular masses, typically beyond 50 000 Da. The NMR technique TROSY (transverse relaxation-optimized spectroscopy) has been developed for studies of structures of this size in solution. In this paper, strategies for the use of TROSY-based NMR experiments with membrane proteins are discussed and illustrated with results obtained with the *Escherichia coli* integral membrane proteins OmpX and OmpA in mixed micelles with the detergent dihexanoylphosphatidylcholine (DHPC). For OmpX, complete sequence-specific NMR assignments have been obtained for the polypeptide backbone. The ^{13}C chemical shifts and nuclear Overhauser effect data then resulted in the identification of the regular secondary structure elements of OmpX/DHPC in solution, and in the collection of an input of conformational constraints for the computation of the global fold of the protein. For OmpA, the NMR assignments are so far limited to about 80% of the polypeptide chain, indicating different dynamic properties of the reconstituted OmpA β-barrel from those of OmpX. Overall, the present data demonstrate that relaxation-optimized NMR techniques open novel avenues for studies of structure, function and dynamics of integral membrane proteins.

Key words: Membrane protein;
Outer membrane protein A from *E. coli*;
Outer membrane protein X from *E. coli*; NMR structure;
Transverse relaxation-optimized spectroscopy;
Isotope labeling

1. Introduction

About 30% of the genes in living organisms are expected to encode membrane proteins [1–3]. Notwithstanding the abundance of this class of proteins and the crucial importance of work in this area, the database of three-dimensional (3D) membrane protein structures is still small [4], reflecting the challenge posed to structural biologists by these molecules. It is generally difficult to obtain crystals of membrane proteins that are suitable for X-ray diffraction studies, and solution NMR spectroscopy [5,6] has until recently only been applied in a few instances for studies of small membrane proteins and membrane protein fragments (for reviews, see [7,8]).

The major problem when studying membrane proteins by solution NMR arises from the fact that they usually need to be incorporated into micelles in order to be solubilized in polar solvents. Suitable mixed micelles for solution NMR should ensure the structural and functional integrity of the membrane protein and at the same time be sufficiently small to allow rapid Brownian motions [5,6,9–11]. In reality, mixed micelles composed of protein and detergent molecules typically have sizes beyond 50 kDa, tumble slowly in solution, and yield broad NMR lines and poor signal-to-noise ratios as a consequence of rapid transverse spin relaxation.

Recent developments in solution NMR techniques made it possible to extend NMR studies to structures in the size range 50–150 kDa and beyond [12,13]. Transverse relaxation-optimized spectroscopy (TROSY) [12] and cross-correlated relaxation-enhanced polarization transfer (CRINEPT) [13], combined with deuterium isotope labeling [14], reduce transverse relaxation rates, and as a result yield improved spectra with narrower linewidths and higher signal-to-noise ratio. For studies of large structures, the incorporation of TROSY elements into the triple-resonance NMR experiments that are commonly used for the sequential assignment of ^{13}C,^{15}N-labeled proteins [15–18] results in sensitivity gains of one to two orders of magnitude when compared to the corresponding conventional triple-resonance experiments. This now enables measurements of high-quality multidimensional NMR spectra and obtaining complete sequence-specific backbone resonance assignments for proteins in structures of size 100 kDa and beyond [19].

The complexity of the NMR spectra increases with the size of the molecule studied and the concomitant spectral crowding may limit the extent of the spectral analysis. Therefore, the

*Corresponding author. Fax: (41)-1-633 1151.
E-mail address: cesar@mol.biol.ethz.ch (C. Fernández).

[1] Present address: Laboratory of Physical Chemistry, Eidgenössische Technische Hochschule Zürich, CH-8092 Zürich, Switzerland.

Abbreviations: 2D, two-dimensional; 3D, three-dimensional; COSY, correlation spectroscopy; DHPC, dihexanoylphosphatidylcholine (1,2-dihexanoyl-*sn*-glycero-3-phosphocholine); DPC, dodecylphosphocholine; NOE, nuclear Overhauser effect; NOESY, NOE spectroscopy; OmpA, outer membrane protein A from *E. coli*; OmpX, outer membrane protein X from *E. coli*; ppm, parts per million; TROSY, transverse relaxation-optimized spectroscopy

0014-5793/01/$20.00
PII: S0014-5793(01)02742-9

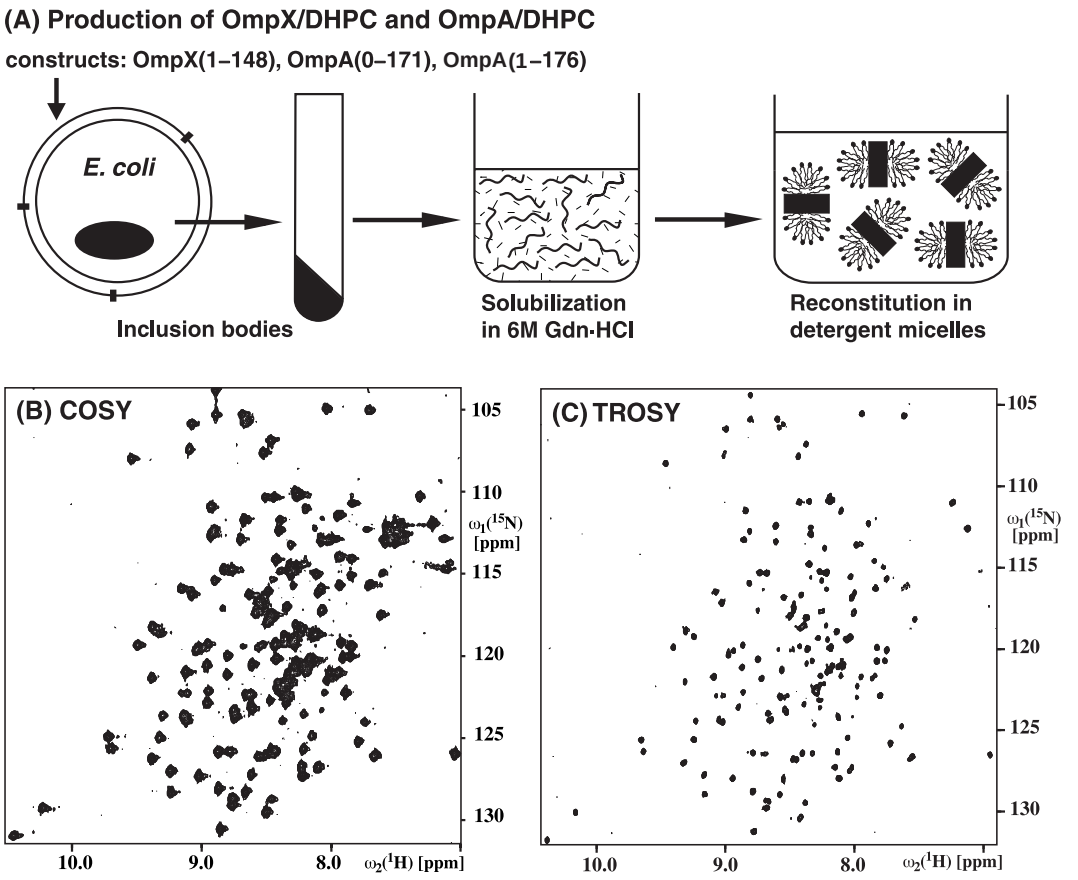

Fig. 1. A: Survey of the production of the OmpX/DHPC and OmpA/DHPC samples used for our NMR studies. For details see [30]. B,C: Contour plots of $^{15}N,^{1}H$ correlation spectra measured with $^{2}H,^{13}C,^{15}N$-labeled OmpX in mixed micelles with DHPC at a ^{1}H resonance frequency of 750 MHz and at 30°C. B: Conventional 2D [$^{15}N,^{1}H$]-COSY. C: 2D [$^{15}N,^{1}H$]-TROSY. The two spectra were identically recorded and processed. Gdn·HCl, guanidine hydrochloride.

preferred current use of relaxation-optimized NMR techniques is with large structures that yield relatively simple spectra, such as homo-oligomeric proteins [20–23]. For systems without symmetrical repeats, novel selective labeling strategies [14,24,25] have already been introduced, in particular segmental isotope labeling [26,27], which are, however, technically demanding and rather expensive. With membrane proteins solubilized in detergent micelles, uniform ^{13}C and ^{15}N labeling of the polypeptide chain ensures that the protein NMR signals can be detected with little or no interference from the signals of the unlabeled detergent molecules, even though these may represent a large fraction of the usually large overall mass of the mixed micelles. Fortunately, important progress has been made in membrane protein overexpression, purification and refolding [28,29], since high yield expression of proteins is essential for producing isotope-labeled reconstituted membrane proteins at reasonable cost.

This paper illustrates the use of solution NMR spectroscopy for studies of membrane proteins with investigations of the outer membrane protein OmpX from *Escherichia coli* in 60 kDa OmpX/dihexanoylphosphatidylcholine (DHPC) micelles [30], and the transmembrane domain of the *E. coli* outer membrane protein OmpA in mixed micelles with DHPC [31] or with dodecylphosphocholine (DPC) [32]. In our laboratory, OmpX and OmpA were selected for these studies because they had previously been well characterized by X-ray crystallography [33–35] and by physicochemical techniques, which enabled reliable controls of the progress made in the NMR method development.

2. The outer membrane proteins OmpX and OmpA from *E. coli*

OmpX and OmpA are integral membrane proteins. The 148-residue, single-domain protein OmpX promotes cell adhesion and invasion of host cells and is involved in defense against the complement systems of the host [33,36,37]. OmpA consists of a transmembrane domain with residues 1–171 and a soluble domain of residues 172–325. OmpA is involved in bacterial conjugation, acts as a receptor for bacteriophages, mediates virulence and pathogenicity, and is an integral part of the membrane structure [34,35,38].

The crystal structures of OmpX and of the transmembrane domain of OmpA in the presence of the detergent *n*-octyltetraoxyethylene both consist of an eight-stranded, antiparallel β-barrel, in which successive pairs of β-strands are connected to each other by tight turns at the periplasmic side of the barrel, and by more extensive loops at the extracellular end [33–35]. A notable difference between the two structures, apart from the different overall dimensions, is that OmpA contains significantly longer extracellular loops. In the OmpA crystal structure, three of the four extracellular loops were not observed in the electron density maps [34,35]. OmpX contains

well-defined extensions of four of the eight strands in the β-barrel in locations corresponding to the aforementioned disordered loops in OmpA [33].

For the NMR studies in our laboratory, OmpX and OmpA were overexpressed in inclusion bodies in *E. coli* (Fig. 1A). The yields after purification and reconstitution in DHPC micelles were about 15 mg of protein per liter of minimal medium in 99% D_2O. The final NMR sample composition was as follows: protein concentration 2 mM, mixed solvent of 97% H_2O/3% D_2O containing 20 mM phosphate buffer at pH 6.8, 100 mM NaCl and 300 mM DHPC. The sample temperature was 30°C. Under these conditions, we estimated the molecular mass of the mixed micelles of OmpX/DHPC to be of the order of 60 kDa, and of OmpA/DHPC of the order of 80 kDa, based on a variety of NMR measurements and other physicochemical studies (to be published). We decided on these experimental conditions after an extensive search for parameters that would yield optimal NMR sensitivity and resolution, which also included several different types of detergents (to be published).

3. NMR assignments, collection of conformational constraints and structure calculations with OmpX

Fig. 1 shows spectra measured with a $^{2}H,^{13}C,^{15}N$-labeled sample of OmpX in mixed micelles with unlabeled DHPC. As expected for particles of this size, the use of TROSY resulted in a significant improvement of the correlation experiment [12], and application of the TROSY technique yielded high-quality triple-resonance spectra (Fig. 2A); as shown elsewhere [30], a 10-fold sensitivity gain was obtained on average in the 3D [$^{15}N,^{1}H$]-TROSY-HNCA experiment [15] when compared

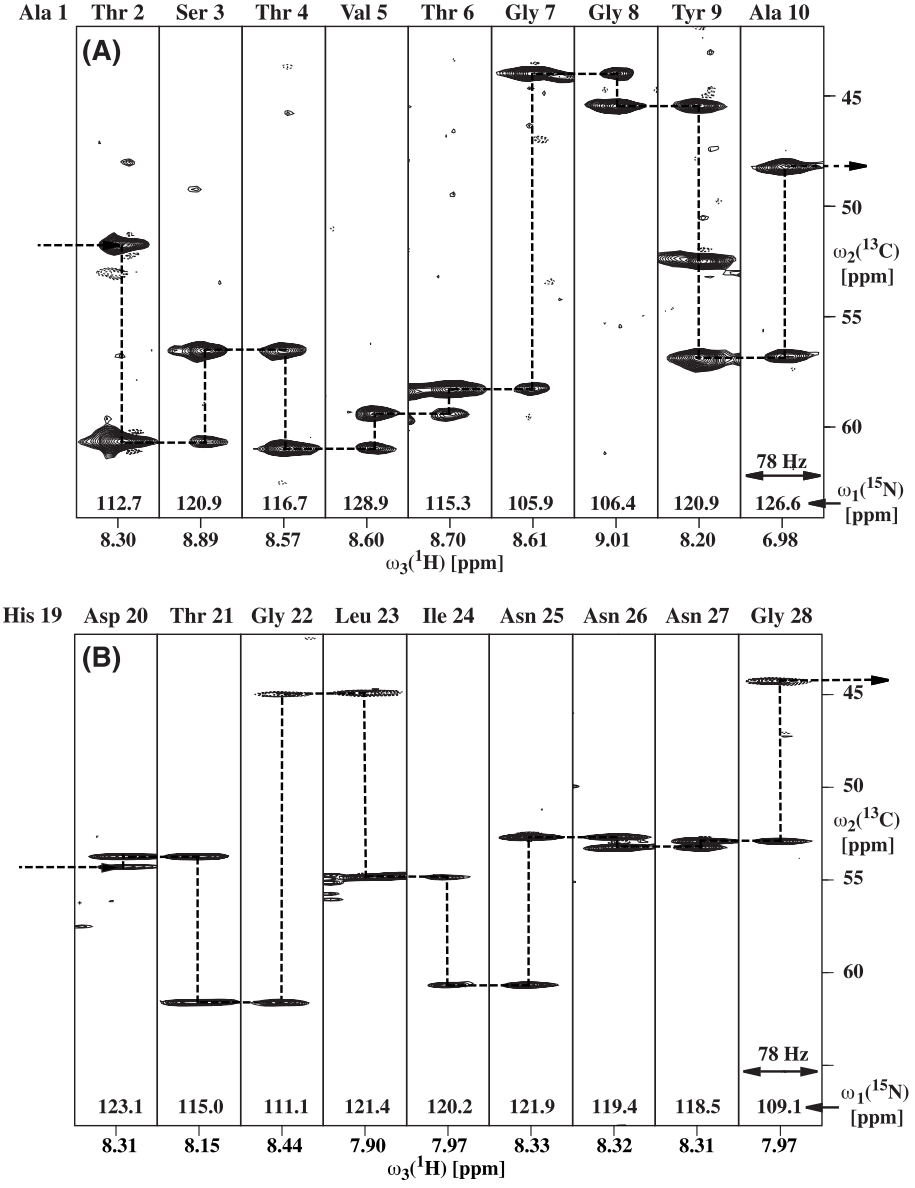

Fig. 2. A: 3D [$^{15}N,^{1}H$]-TROSY-HNCA spectrum measured with OmpX/DHPC. B: 3D [^{13}C]-*ct*-[$^{15}N,^{1}H$]-TROSY-HNCA spectrum recorded with OmpA(0–171)/DHPC. The spectra are presented in the form of [$\omega_2(^{13}C),\omega_3(^{1}H)$] strips. At the top of each strip, the sequence-specific assignment is indicated by the amino acid symbol and the sequence position. The strips were taken at the ^{15}N chemical shifts indicated at the bottom of the strips, and are centered about the corresponding $^{1}H^{N}$ chemical shifts. Horizontal and vertical broken lines connect the intraresidual and sequential HNCA connectivities, and thus outline the sequential assignment pathway.

Fig. 3. A: Survey of the extent of the sequential NMR assignments obtained for OmpX/DHPC. The assignments are mapped onto a ribbon representation of the X-ray crystal structure of OmpX [33], using the following color code: red, assigned residues that are located in well structured regions; yellow, assigned residues that are located in flexibly disordered loops. The chain ends are identified with 'N' and 'C'. B: NMR structure of OmpX represented by a superposition of 20 energy-refined DYANA conformers for pairwise global best fit of the N, C^{α} and C′ backbone atoms of the β-sheet. The input for the structure calculation consisted of 107 NOE upper distance restraints between backbone amide protons, 400 hydrogen bond constraints (200 upper limit and 200 lower limit distance constraints) [47] between residues located in adjacent β-strands, and 172 dihedral angle constraints on φ and ψ obtained by reference to the protein data bank with the program TALOS [48]. C: Stereo view of a similar presentation of the NMR structure of OmpX/DHPC [30] calculated using only the directly accessible experimental constraints as input data, i.e. 107 NOE upper distance restraints between backbone amide protons and 140 dihedral angle constraints on φ and ψ from ^{13}C chemical shifts. D: Extent of the sequential NMR assignments obtained for OmpA(0–171)/DHPC. Same presentation as in A, using the crystal structure of OmpA [34,35]; color code: red, assigned residues in structured regions of the polypeptide chain; yellow, assigned residues in flexibly disordered loops (three of the four loops were 'X-ray-invisible'); blue, unassigned, NMR-invisible; green, residues showing two sets of resonances ('doubling'). E: Same presentation as in D for OmpA(1–176)/DHPC. The figures have been prepared with the program MOLMOL [54].

→

to the conventional 3D HNCA spectrum [39]. Collection of a complete set of $^{13}C^{\alpha}$ and $^{13}C^{\beta}$ chemical shifts (Fig. 3A) from TROSY-type triple-resonance spectra resulted in the identification of the positions of the eight β-strands in the amino acid sequence [30]. Furthermore, neighboring β-strands could be unambiguously identified using long-range $d_{NN}(i,j)$ nuclear Overhauser effects (NOEs) [5] from a 3D [^{1}H,^{1}H]-NOESY-[^{15}N,^{1}H]-TROSY spectrum [40].

Based on a set of 107 experimental NOE-derived $^1H^N$-$^1H^N$ upper limit distance constraints and 140 dihedral angle constraints derived from the $^{13}C^{\alpha}$ chemical shifts [41–45], the three-dimensional structure of OmpX/DHPC was calculated with the torsion angle dynamics protocol of DYANA [46], using the standard procedure commonly employed for soluble proteins. As expected from the limited amount of data, only low precision was achieved, with a global RMSD value relative to the mean coordinates for the β-barrel of 2.0 Å (Fig. 3C), but the polypeptide backbone fold can readily be followed. Inclusion of hydrogen bond constraints [47] and additional dihedral angle constraints obtained using the program TALOS [48] into the input for the structure calculations yielded a significantly better defined set of conformers, with an RMSD value relative to the mean coordinates calculated for the backbone heavy atoms in the β-barrel of 0.9 Å (Fig. 3B). A comparison of the NMR structure with the X-ray structure [33] shows close coincidence of the global backbone fold [30] (see Fig. 3A–C).

4. NMR spectroscopy with OmpA

For OmpA, the experimental conditions as well as the polypeptide construct were varied in attempts to obtain high-quality NMR spectra. For the OmpA transmembrane domain construct containing the residues 0–171, two sets of ^{15}N-$^1H^N$ correlation peaks were observed for about one-fourth of the residues (Fig. 3D), with relative intensities of about 1:1. This peak doubling was seen in three different detergents, i.e. DHPC, *n*-octyl glucoside and *n*-octyltetraoxyethylene. In DHPC micelles it was insensitive to temperature in the range 15–40°C, to variation within the stability range of the mixed micelles of the protein-to-DHPC ratio, to the overall detergent concentration and to pH. All residues showing double resonances are located in the periplasmic half of the barrel, including or surrounding the individual periplasmic turns (Fig. 3D). A second construct containing the residues 1–176 showed only one set of resonances for all observable residues (Fig. 3E). Further studies of the origin of the signal doubling in OmpA(0–171)/DHPC are in progress, including experiments with different detergents.

Using identical experimental conditions as for OmpX/DHPC, sequential resonance assignments have been achieved for about 80% of the polypeptide backbone in both forms of OmpA(0–171)/DHPC as well as in OmpA(1–176)/DHPC (Figs. 2B and 3D,E). For the molecular regions that could be assigned, the results were based on experimental data of comparably high quality to those obtained with OmpX/DHPC (Fig. 2B). The OmpA/DHPC secondary structure was determined from the $^{13}C^{\alpha}$ and $^{13}C^{\beta}$ chemical shifts and from long-range $d_{NN}(i,j)$ NOEs [5] measured with a 3D [^{1}H,^{1}H]-NOESY-[^{15}N,^{1}H]-TROSY spectrum. The ensemble of the data on OmpA/DHPC supports that the antiparallel β-barrel observed in the X-ray crystal structure [34,35] is preserved under the solution conditions of the NMR experiments for both constructs used.

Studies of OmpA were recently also reported by Arora et al. [32]. These authors used a construct of OmpA(0–176) in an aqueous solution containing 600 mM DPC, 10 mM phosphate at pH 6.3 and 50 mM NaCl, which was studied at 50°C. The published data indicate that very similar results were obtained for OmpA(0–176)/DPC as for OmpA(1–176)/DHPC and OmpA(0–171)/DHPC, i.e. backbone assignments were obtained for 138 residues (76%), and the ensemble of the data supports that the crystal structure fold is also maintained in DPC micelles. Intriguingly, two sets of NMR peaks with relative intensities of about 4:1 were seen for all NMR-observable amino acid residues in DPC-solubilized OmpA(0–176).

The unassigned and 'NMR-unobservable' peptide segments form a ring around the β-barrel that separates the well structured, compact core of OmpA from the X-ray-unobservable [34,35], disordered extracellular loops (Fig. 3D,E). This observation could be rationalized by conformational exchange processes of intermediate rates on the NMR time scale, which would cause line broadening in this molecular region [5,6]. This hypothesis appears to be supported by ^{15}N-spin relaxation data (unpublished) and is compatible with the B-factors obtained from X-ray diffraction studies [35], which show a gradual increase of structural disorder from the center of the barrel towards the loops. It is intriguing that similar behavior is observed in micelles with different detergent molecules, which indicates that this phenomenon is characteristic of OmpA rather than the detergent or lipid environment. The same dynamic behavior might thus be maintained in the natural environment of OmpA provided by the lipid bilayer of the outer membrane of *E. coli*. It thus appears of interest for future studies to further investigate possible implications of the dynamics of the β-barrel for the physiological functions of OmpA as a porin, which appears to be subject of continued controversy [34,35,49].

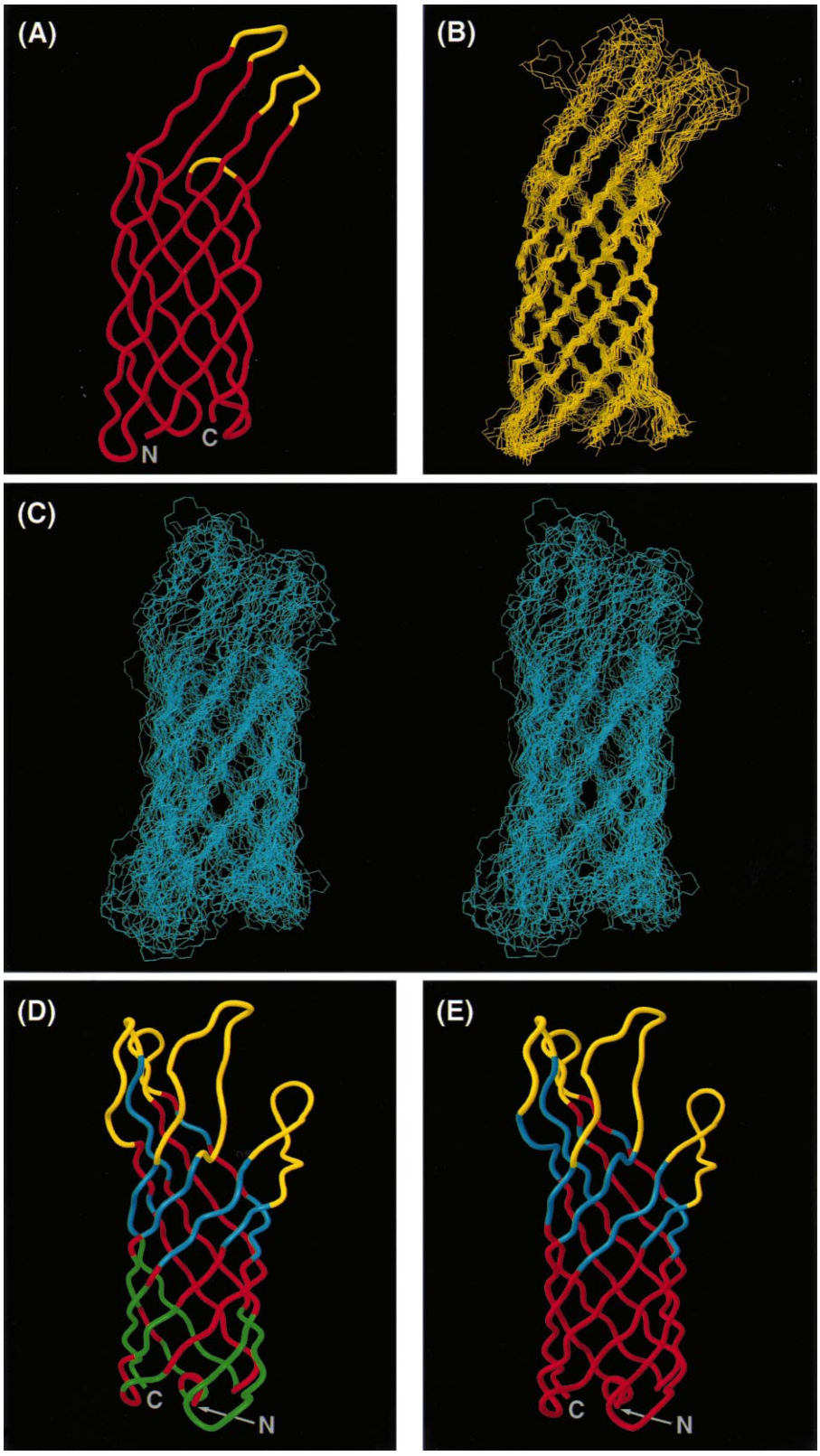

5. Concluding remarks

The results discussed in this paper demonstrate that relaxation-optimized NMR techniques open novel avenues for studies of structure, dynamics and function of integral membrane proteins. As a general comment on work with micelle-reconstituted membrane proteins, it seems useful to repeat that high-quality spectra of the kind shown in Figs. 1 and 2 were obtained after optimizing the conditions for solution NMR by a suitable choice of the detergent, and by adjusting the detergent concentration, the protein–detergent ratio, the salt concentration and the pH value. In the case of OmpA,

optimizing the experimental conditions also included work with multiple polypeptide constructs (Fig. 3D,E) [32]. It can be anticipated that experience on obtaining NMR-favorable preparations of membrane proteins will soon accumulate and lead to efficient production of NMR samples. The method for obtaining sequence-specific backbone assignments should then be generally applicable to proteins of molecular mass up to about 25 kDa, providing a basis for studies of functional aspects [50], of internal mobility [5,6], and similar.

As exemplified by OmpX/DHPC (Fig. 3B,C), the NMR experiments used for complete sequence-specific resonance assignments are also sufficient for a low-precision definition of the fold of β-barrel-type proteins. To further improve the precision of structure determinations for β-proteins, one now needs to investigate to what extent techniques used to obtain additional experimental constraints in soluble proteins can be adapted for use with reconstituted membrane proteins. Examples are resonance assignments of amino acid side chains by selective protonation in otherwise perdeuterated proteins [14], collection of supplementary conformational constraints [5], possibly including residual dipolar couplings [51–53], or chemical shift-based references to protein structure data banks (e.g. [48]). In principle, the same applies with regard to structure determination of α-helical membrane proteins, or membrane-associated polypeptides without regular secondary structure, but for these classes of proteins one will first need to develop procedures that enable an unambiguous determination of the global fold.

Acknowledgements: We thank P. Güntert for help with the structure calculation of Fig. 3B, J. Vogt and G.E. Schulz for providing plasmids used for the production of OmpX and OmpA, and Mrs. M. Geier for the careful processing of the manuscript. Financial support was obtained from the Schweizerischer Nationalfonds (Project 31.49047.96).

References

[1] Walker, J.E. and Saraste, M. (1996) Curr. Opin. Struct. Biol. 6, 457–459.
[2] Kühlbrandt, W. and Gouaux, E. (1999) Curr. Opin. Struct. Biol. 9, 445–447.
[3] Bowie, J. (2000) Curr. Opin. Struct. Biol. 10, 435–437.
[4] Berman, H.M., Westbrook, J., Feng, Z., Gilliland, G., Bhat, T.N., Weissig, H., Shindyalov, I.N. and Bourne, P.E. (2000) Nucleic Acids Res. 28, 235–242.
[5] Wüthrich, K. (1986) NMR of Proteins and Nucleic Acids, Wiley, New York.
[6] Cavanagh, J., Fairbrother, W.J., Palmer III, A.G. and Skelton, N.J. (1996) Protein NMR Spectroscopy. Principles and Practice, Academic Press, New York.
[7] Opella, S.J. (1997) Nat. Struct. Biol. 4, 845–848.
[8] Marassi, F.M. and Opella, S.J. (1998) Curr. Opin. Struct. Biol. 8, 640–648.
[9] McDonnell, P.A. and Opella, S. (1993) J. Magn. Reson. B 102, 120–125.
[10] Vinogradova, O., Sönnichsen, F. and Sanders II, C.R. (1998) J. Biomol. NMR 11, 381–386.
[11] Sanders, C.R. and Oxenoid, K. (2000) Biochim. Biophys. Acta 1508, 129–145.
[12] Pervushin, K., Riek, R., Wider, G. and Wüthrich, K. (1997) Proc. Natl. Acad. Sci. USA 94, 12366–12371.
[13] Riek, R., Wider, G., Pervushin, K. and Wüthrich, K. (1999) Proc. Natl. Acad. Sci. USA 96, 4918–4923.
[14] Gardner, K.H. and Kay, L.E. (1998) Annu. Rev. Biophys. Biomol. Struct. 27, 357–406.
[15] Salzmann, M., Pervushin, K., Wider, G., Senn, H. and Wüthrich, K. (1998) Proc. Natl. Acad. Sci. USA 95, 13585–13590.
[16] Salzmann, M., Pervushin, K., Wider, G., Senn, H. and Wüthrich, K. (1999) J. Biomol. NMR 14, 85–88.
[17] Salzmann, M., Wider, G., Pervushin, K. and Wüthrich, K. (1999) J. Biomol. NMR 15, 181–184.
[18] Salzmann, M., Wider, G., Pervushin, K., Senn, H. and Wüthrich, K. (1999) J. Am. Chem. Soc. 121, 844–848.
[19] Salzmann, M., Pervushin, K., Wider, G., Senn, H. and Wüthrich, K. (2000) J. Am. Chem. Soc. 122, 7543–7548.
[20] Wüthrich, K. (1998) Nat. Struct. Biol. 5, 492–495.
[21] Wider, G. and Wüthrich, K. (1999) Curr. Opin. Struct. Biol. 9, 594–601.
[22] Riek, R., Pervushin, K. and Wüthrich, K. (2000) Trends Biochem. Sci. 25, 462–468.
[23] Pervushin, K. (2000) Q. Rev. Biophys. 33, 161–197.
[24] Goto, N.K., Gardner, K.H., Mueller, G.A., Millis, R.C. and Kay, L.E. (1999) J. Biomol. NMR 13, 369–374.
[25] Arrowsmith, C.H., Pachter, R., Altman, R.B., Iyer, S.B. and Jardetzki, O. (1990) Biochemistry 29, 6332–6341.
[26] Yamazaki, T., Otomo, T., Oda, N., Kyogoku, Y., Uegaki, K., Ito, N., Ishino, Y. and Nakamura, H. (1998) J. Am. Chem. Soc. 120, 5591–5592.
[27] Xu, R., Ayers, B., Cowburn, D. and Muir, T.W. (1999) Proc. Natl. Acad. Sci. USA 96, 388–393.
[28] Griesshammer, R. and Tate, C.G. (1995) Q. Rev. Biophys. 28, 315–422.
[29] Von Jagow, G. and Scägger, H., Eds. (1994) A Practical Guide to Membrane Protein Purification, Academic Press, New York.
[30] Fernández, C., Adeishvili, K. and Wüthrich, K. (2001) Proc. Natl. Acad. Sci. USA 98, 2358–2363.
[31] Fernández, C., Hilty, C., Bonjour, S., Pervushin, K. and Wüthrich, K. (2001) in: Proceedings of the International Conference on Structure, Dynamics and Function of Proteins in Biological Membranes, Ascona, 13–17 March 2001, PSI, Switzerland, p. 53.
[32] Arora, A., Abildgaard, F., Bushweller, J.H. and Tamm, L. (2001) Nat. Struct. Biol. 8, 334–338.
[33] Vogt, J. and Schulz, G.E. (1999) Structure 7, 1301–1309.
[34] Pautsch, A. and Schulz, G.E. (1998) Nat. Struct. Biol. 5, 1013–1017.
[35] Pautsch, A. and Schulz, G.E. (2000) J. Mol. Biol. 298, 273–282.
[36] de Kort, G., Bolton, A., Martin, G., Stephen, J. and van de Klundert, J.A.M. (1994) Infect. Immun. 62, 4722–4726.
[37] Stoorvogel, J., van Bussel, M.J.A.W.M. and van de Klundert, J.A.M. (1987) FEMS Microbiol. Lett. 48, 277–281.
[38] Koebnik, R. (1995) in: The Encyclopedia of Molecular Biology, Wiley, New York.
[39] Grzesiek, S. and Bax, A. (1992) J. Magn. Reson. 96, 432–440.
[40] Pervushin, K., Braun, D., Fernández, C. and Wüthrich, K. (2000) J. Biomol. NMR 17, 195–202.
[41] Spera, S. and Bax, A. (1991) J. Am. Chem. Soc. 113, 5490–5492.
[42] Wishart, D.S., Sykes, B.D. and Richards, F.M. (1991) J. Mol. Biol. 222, 311–333.
[43] Wishart, D.S. and Sykes, B.D. (1994) J. Biomol. NMR 4, 171–180.
[44] Luginbühl, P., Szyperski, T. and Wüthrich, K. (1995) J. Magn. Reson. 109, 229–233.
[45] Metzler, W.J., Constantine, K.L., Friedrichs, M.S., Bell, A.J., Ernst, E.G., Lavoie, T.B. and Mueller, L. (1993) Biochemistry 32, 13818–13829.
[46] Güntert, P., Mumenthaler, C. and Wüthrich, K. (1997) J. Mol. Biol. 273, 283–298.
[47] Williamson, M.P., Havel, T.F. and Wüthrich, K. (1985) J. Mol. Biol. 182, 295–315.
[48] Cornilescu, G., Delaglio, F. and Bax, A. (1999) J. Biomol. NMR 13, 289–302.
[49] Arora, A., Rinehart, D., Szabo, G. and Tamm, L.K. (2000) J. Biol. Chem. 275, 1594–1600.
[50] Shuker, S.B., Hajduk, P.J., Meadows, R.P. and Fesik, S.W. (1996) Science 274, 1531–1534.
[51] Tolman, J.R., Flanagan, J.M., Kennedy, M.A. and Prestegard, J.H. (1995) Proc. Natl. Acad. Sci. USA 92, 9279–9283.
[52] Tjandra, N. and Bax, A. (1997) Science 278, 1111–1114.
[53] Prestegard, J.H., Al-Hashimi, H.M. and Tolman, J.R. (2000) Q. Rev. Biophys. 33, 371–424.
[54] Koradi, R., Billeter, M. and Wüthrich, K. (1996) J. Mol. Graph. 14, 51–55.